INTERNATIONAL JOURNAL FOR NUMERICAL METHODS IN FLUIDS
Int. J. Numer. Meth. Fluids 2005; **47**:863–869
Published online 29 December 2004 in Wiley InterScience (www.interscience.wiley.com). DOI: 10.1002/fld.857

A semi-implicit method conserving mass and potential vorticity for the shallow water equations on the sphere

Luca Bonaventura[1,*,†], Luis Kornblueh[1], Thomas Heinze[2] and Pilar Ripodas[2]

[1]*Max Planck Institut für Meteorologie, Bundesstraße 53, 20146, Hamburg, Germany*
[2]*Deutscher Wetterdienst, Kaiserleistraße 42, 63067, Offenbach, Germany*

SUMMARY

A semi-implicit discretization for the shallow water equations is discussed, which uses triangular Delaunay cells on the sphere as control volumes and conserves mass and potential vorticity. The geopotential gradient, the Coriolis force terms and the divergence of the velocity field are discretized implicitly, while an explicit time discretization is used for the non-linear advection terms. The results obtained with a preliminary implementation on some idealized test cases are presented, showing that the main features of large scale atmospheric flows are well represented by the proposed method. Copyright © 2004 John Wiley & Sons, Ltd.

KEY WORDS: shallow water equations; semi-implicit methods; icosahedral grid; vorticity preserving methods; Delaunay triangulations

1. INTRODUCTION

A semi-implicit discretization for the shallow water equations is discussed, which uses the triangular cells of a Delaunay triangulation on the sphere as control volumes. A preliminary version of the same method was introduced in Reference [1]. The discrete model variables are the velocity components normal to the cell sides and the cell averaged values of the geopotential height, so that the method can be seen as an extension of the C-grid staggering on quadrilateral grids (see e.g. References [2, 3]) to triangular grids. The Raviart–Thomas finite element of order zero (see e.g. References [4, 5]) is used to reconstruct a uniquely defined velocity field from the velocity components normal to the cell sides. The geopotential gradients, the Coriolis force terms and the divergence of the velocity field are discretized implicitly, while an explicit time discretization is used for the non-linear advection terms. The resulting numerical method conserves mass and potential vorticity by construction. Results

*Correspondence to: Luca Bonaventura, Max Planck Institut für Meteorologie, Bundesstraße 53, 20146, Hamburg, Germany.
†E-mail: bonaventura@dkrz.de

Received 27 April 2004
Revised 12 August 2004
Accepted 17 August 2004

obtained with a preliminary implementation on a quasi-uniform icosahedral grid demonstrate the effective accuracy of the proposed method and its potential for application to general circulation models. Finite element approaches based on such geodesic grids have been introduced in References [6, 7]. Finite volume approaches were instead presented in References [8–10]. Usually, the hexagonal and pentagonal cells of Voronoi tessellations have been used as control volumes. However, triangular control volumes allow for much simpler construction of mass conservative models on hierarchies of locally refined grids, along the lines of the cartesian mesh refinement approaches (see e.g. References [11, 12]).

2. THE SHALLOW WATER EQUATIONS AND THE NUMERICAL METHOD

The vector invariant form of the shallow water equations on the sphere is considered:

$$\frac{\partial \mathbf{u}}{\partial t} = -(\zeta + f)\mathbf{k} \times \mathbf{u} - \nabla(gh + K) \tag{1}$$

$$\frac{\partial h}{\partial t} + \nabla \cdot (h^* \mathbf{u}) = 0 \tag{2}$$

Here $\mathbf{u}$ is the horizontal velocity vector (on the sphere), $K = |\mathbf{u}|^2/2$ is the kinetic energy, ζ is the vertical component of the relative vorticity, f is the Coriolis coefficient, h^* is the fluid depth, $h = h^* + h^s$ is the height of the free surface above mean sea level, h_s is the height of the orography, g is the gravitational constant and $\mathbf{k}$ the unit vector in the radial outward direction.

The proposed discretization methods is defined on a special case of Delaunay triangulation on the sphere, the icosahedral geodesic grid described, e.g. in Reference [8], which is obtained by dyadic refinement of the regular icosahedron. Although we will only refer to the icosahedral grid in the following, the method can be easily generalized on more general Delaunay triangulations, under mild regularity assumptions (see e.g. Reference [13]). The icosahedral construction yields a Delaunay triangulation of the sphere to which a Voronoi tessellation is naturally associated (see e.g. Reference [14] and the references therein for a complete description of Delaunay–Voronoi grid pairs on the sphere), which consists of convex spherical

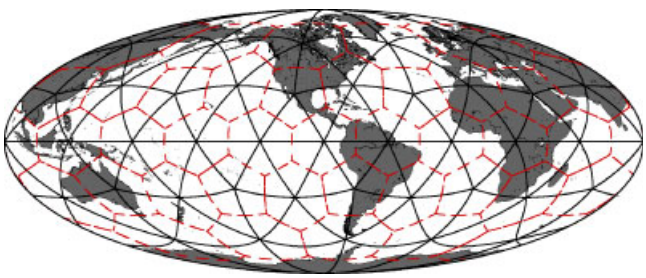

Figure 1. Delaunay triangulation (solid lines) and Voronoi tessellation (dashed lines) on the sphere, as obtained by dyadic refinement of the regular icosahedron.

polygons (either pentagons or hexagons, see Figure 1). The points of the icosahedral grid obtained in this way constitute the Voronoi grid on the sphere. Each of them belongs to a single hexagonal or pentagonal cell. The vertices of these polygons constitute the dual, or Delaunay grid. The Delaunay cells of the icosahedral grid are all triangles. For each side of a Voronoi cell, there is a unique orthogonal side of the Delaunay cell associated to it.

Some notation to describe the grid topology and geometry will now be introduced. Let i denote the generic cell of the Delaunay grid. Let $\mathscr{E}(i)$ denote the set of all edges of cell i and $\mathscr{C}(i)$ the set of all cells that have edges in common with cell i. The gridpoint associated to cell i will also be referred to as the cell centre. The generic vertex of a cell, which is also the centre of a cell in the dual grid, is denoted by v. $\mathscr{C}(v)$ denotes the set of all cells of which v is a vertex and $\mathscr{E}(v)$ denotes the set of all edges of the dual cell whose centre is vertex v. The area of cell i is denoted by A_i, while the area of the dual cell is denoted by A_v. Let l denote the generic edge of a cell. The length of the edge l of a cell is denoted by λ_l and the distance between the centres of the cells adjacent to edge l is denoted by δ_l. At each edge, a unit vector $\mathbf{N}_l$ normal to the edge l is assigned. $\mathbf{T}_l$ denotes the unit vector tangential to the edge l, chosen in such a way that $\mathbf{N}_l \times \mathbf{k}_l = \mathbf{T}_l$ holds, where $\mathbf{k}_l$ denotes the radial outgoing unit vector perpendicular to the tangent plane at the intersection of the primal and the dual edge l. Furthermore, for each cell edge, the unit vector pointing in the outer normal direction with respect to cell i is denoted by $\mathbf{n}_{i,l}$. Unit vectors $\mathbf{n}_{v,l}$ are also introduced, as pointing in the outer normal direction with respect to the dual cell v. The corresponding tangential vectors $\mathbf{t}_{v,l}$ are defined so that $\mathbf{n}_{v,l} \times \mathbf{t}_{v,l} = \mathbf{k}_l$. It can be seen that, by simple geometric arguments, one has $\mathbf{N}_l \cdot \mathbf{t}_{v,l} = \mathbf{T}_l \cdot \mathbf{n}_{v,l}$.

In order to develop an analogue of the rectangular C-type staggering (see e.g. Reference [2]) on the Delaunay grids, the *mass points* are defined as the centres of the grid cells, while the *velocity points* are defined for each cell edge as the intersection between the edges of the Voronoi and Delaunay cells (see Figure 1). In a C-grid discretization approach, the discrete prognostic variables considered are the value of the height field h_i at the mass points (interpreted as a cell averaged value) and the normal velocity components u_l. The tangential velocity components, which are needed, e.g. for the computation of the Coriolis force term, must be reconstructed. Given the edge l of a cell, the adjacent cells are denoted by the indexes $i(l,1)$ and $i(l,2)$. Vertex indexes $v(l,1)$ and $v(l,2)$ can also be defined analogously. Given a generic discrete vector field $\mathbf{g}$ on the sphere, its value at a velocity point can be represented as $\mathbf{g}_l = g_l \mathbf{N}_l + \hat{g}_l \mathbf{T}_l$, where g_l and $\hat{g}_l$ denote the normal and the tangential components, respectively.

Given these definitions, discrete operators can be introduced, which will then be employed to define the proposed numerical algorithm. The directional derivatives in the normal and tangential directions are easily approximated as

$$(\delta_\nu h)_l = (h_{i(l,2)} - h_{i(l,1)})/\delta_l, \qquad (\delta_\tau h)_l = (h_{v(l,2)} - h_{v(l,1)})/\lambda_l \tag{3}$$

The discrete divergence and curl operator can also be naturally defined as follows:

$$\mathrm{div}(\mathbf{g})_i = \frac{1}{A_i} \sum_{l \in \mathscr{E}(i)} g_l \mathbf{N}_l \cdot \mathbf{n}_{i,l} \lambda_l, \qquad \mathrm{curl}(\mathbf{g})_v = \frac{1}{A_v} \sum_{l \in \mathscr{E}(v)} g_l \mathbf{N}_l \cdot \mathbf{t}_{v,l} \delta_l \tag{4}$$

The spatial discretization of the continuity equation (2) is then given by

$$A_i \frac{\partial h_i}{\partial t} = - A_i \,\mathrm{div}(\bar{h}^* \mathbf{u})_i \tag{5}$$

where $\bar{h}_l^*$ denotes the arithmetic average of the layer thickness values in the neighbouring cells. The discrete momentum equation can be derived by taking the scalar product of Equation (1) with the unit vector $\mathbf{N}_l$ at a generic velocity point. This yields the equation

$$\frac{\partial u_l}{\partial t} = - (\bar{\zeta}_l + f_l) v_l - \delta_v [gh + K]_l \tag{6}$$

Here, v_l is an approximation of the tangential velocity component, $\zeta_v = \mathrm{curl}(\mathbf{u})_v$ and $\bar{\zeta}_l$ is the arithmetic average of the absolute vorticity values at the ends of the cell edge. An analogous equation can be derived for the tangential velocity component. The Raviart–Thomas finite element of order zero (see e.g. References [4, 5]) is used to reconstruct at each cell centre i a uniquely defined velocity field from the velocity components normal to the cell sides. An important feature of this type of spatial discretizations is that taking the discrete curl of Equation (6) yields automatically a consistent discretization of the relative vorticity equation. It is to be stressed that the same result can be achieved on any dual Voronoi–Delaunay pair. Staggered grid discretizations on quadrilateral grids also displaying this property have been introduced in References [3, 15]. A spatially discretized version of the potential vorticity conservation theorem can also be derived from this property.

A two time level semi-implicit time discretization of Equations (1) and (2) is then given by

$$u_l^{n+1} = u_l^n - \Delta t (f_l + \tilde{\zeta}_l^{n+\alpha}) v_l^{n+\alpha} - \Delta t [\delta_v (g h^{n+\alpha} + \tilde{K}^{n+\alpha})]_l \tag{7}$$

$$A_i h_i^{n+1} = A_i h_i^n - \Delta t A_i \,\mathrm{div}(\bar{h}^* \mathbf{u}^{n+\alpha})_i \tag{8}$$

Here, $\phi^{n+\alpha} = \alpha \phi^{n+1} + (1-\alpha)\phi^n$, $h_l^* = h_l^n - h_l^s$ and $\alpha \in [\frac{1}{2}, 1]$ for stability, with $\alpha = \frac{1}{2}$ yielding a second-order accurate time discretization in the linear case. On the other hand, $\tilde{\psi}^{n+\alpha}$ denotes some estimate of the value of ψ at time $(n+\alpha)\Delta t$ obtained by an explicit discretization. Along the lines of Reference [5], where a more advanced flux form semi-lagrangian scheme was applied in an analogous step, a simple upwind discretization is employed in this preliminary implementation for these intermediate updates. Since the discrete values of ζ are naturally defined at the vertices of the triangular cells, the intermediate update of ζ is computed by a discretization using as control volumes the dual hexagonal/pentagonal cells. The value of the tangential velocity component at time step $n+1$ can be eliminated by deriving the analogue of Equation (6) for the tangential velocity component. The discrete wave equation can then be written as

$$A_i h_i^{n+1} - g\alpha^2 \Delta t^2 A_i \,\mathrm{div}[((\delta_v h^{n+1}) - \alpha \Delta t (f + \tilde{\zeta}^{n+\alpha})(\delta_\tau h^{n+1}))\gamma h^*]_i = \mathscr{F}_i^n(h) \tag{9}$$

$$\mathscr{F}_i^n(h) = A_i h_i^n - (1-\alpha)\Delta t A_i \,\mathrm{div}(h^* \mathbf{u}^n)_i - \alpha \Delta t A_i \,\mathrm{div}(h^* \gamma \mathscr{F}^n(\mathbf{u}))_i$$

$$\mathscr{F}_l^n(\mathbf{u}) = u_l^n - \Delta t(f_l + \tilde{\zeta}_l^{n+\alpha})v_l^n - \alpha(1-\alpha)\Delta t^2(f_l + \tilde{\zeta}_l^{n+\alpha})^2 u_l^n$$
$$- (1-\alpha)\Delta t(\delta_v g h^n)_l - \Delta t(\delta_v \tilde{K}^{n+\alpha})_l$$
$$+ \alpha(1-\alpha)\Delta t^2(f_l + \tilde{\zeta}_l^{n+\alpha})(\delta_\tau g h^n)_l + \alpha\Delta t^2(f_l + \tilde{\zeta}_l^{n+\alpha})(\delta_\tau \tilde{K}^{n+\alpha})_l \quad (10)$$

where $\gamma_l = 1/(1 + \alpha^2\Delta t^2(f_l + \tilde{\zeta}_l^{n+\alpha})^2)$. The set of all Equations (9) for each cell i yields a linear system in the unknowns h_i^{n+1}. Its matrix is sparse and its symmetric part is positive definite and diagonally dominant, which allows for efficient solution even when using relatively simple solvers. Once the values of h_i^{n+1} have been computed, they are back substituted in Equation (7) to obtain the final update of the discrete velocities.

3. NUMERICAL TESTS

Test cases proposed in the standard shallow water test suite [16] have been run with the currently available, preliminary implementation. Since no complete normal mode and stability analysis is available so far, no explicit diffusion was employed in our numerical experiments in order to assess the effective stability and robustness of the proposed method. Values of the implicitness parameter were taken to be in the range $[0.55, 0.57]$. The correct qualitative behaviour of the computed solutions is shown in Figure 2, for test cases 5 and 6. As common in low-order models using grids that are not symmetrical across the equator (see e.g. the discussion in Reference [10]), an asymmetry develops in the solution of test case 6 on longer time scales.

A full quantitative assessment of the accuracy of the proposed method is presently being undertaken. Only preliminary results are shown here with this respect. For test case 5 a reference solution was obtained with a spectral transform model. For this purpose, the spectral transform model of Reference [17] was revised and upgraded to *fortran90*. The reference

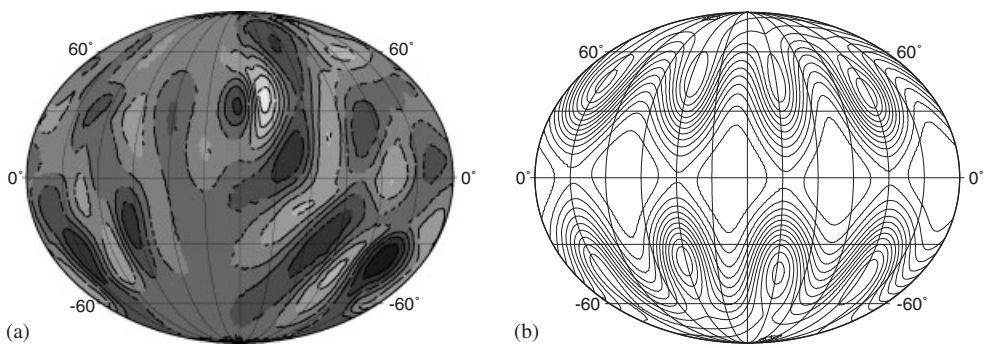

Figure 2. (a) Relative vorticity at day 15 in test case 5. Results were computed on grid level 6 with $\Delta t = 450$ s. Contour lines spacing is $10^{-5}\,\mathrm{s}^{-1}$; and (b) height field at day 15 in test case 6. Results were computed on grid level 6 with $\Delta t = 225$ s. Contour lines spacing is 100 m.

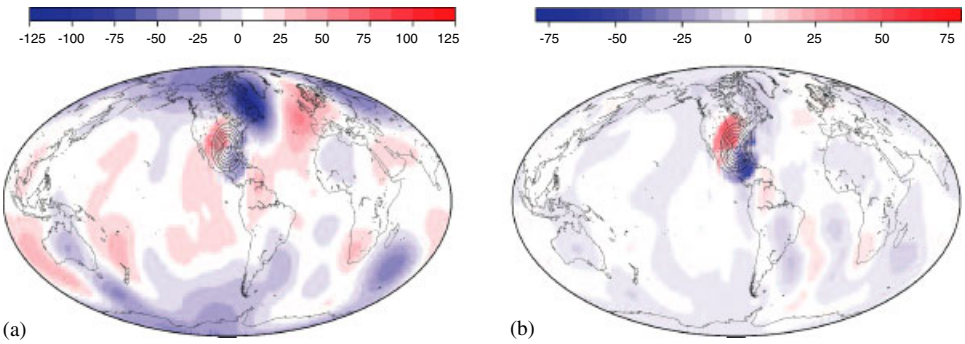

Figure 3. Height field error at day 15 in test case 5, computed on grid level 6 with $\Delta t = 900\,\mathrm{s}$ and on grid level 7 with $\Delta t = 90\,\mathrm{s}$. Black lines denote the orographic contours.

solution was computed at spectral resolution of T213 with a time step of $\Delta t = 90\,\mathrm{s}$. In this test a mountain profile with discontinuous derivatives is introduced in a balanced zonal flow at the initial time. The spectral reference solution is noisy close to the mountain and l_∞ convergence can only be achieved away from the mountain. Plots of the height field error at day 15 are shown in Figure 3 on grid level 6 with $\Delta t = 900\,\mathrm{s}$ and on grid level 7 with $\Delta t = 90\,\mathrm{s}$. It can be observed that, increasing time and space resolution, errors decrease throughout the computational domain away from the mountain.

REFERENCES

1. Bonaventura L. Development of the ICON dynamical core: modelling strategies and preliminary results. In *Proceedings of the ECMWF Workshop on Modelling and Assimilation for the Stratosphere and Tropopause*, Hortal M, Simmons A (eds). ECMWF, Reading, MA, 2003.
2. Arakawa A, Lamb V. A potential enstrophy and energy conserving scheme for the shallow water equations. *Monthly Weather Review* 1981; **109**:18–136.
3. Sadourny R. The dynamics of finite difference models of the shallow water equations. *Journal of Atmospheric Sciences* 1975; **32**:680–689.
4. Quarteroni A, Valli A. *Numerical Approximation of Partial Differential Equations.* Springer: Berlin, 1994.
5. Raviart PA, Thomas JM. A mixed finite element method for 2nd order elliptic problems. In *Mathematical Aspects of Finite Element Methods*, Galligani I, Magenes E (eds), Lecture Notes in Mathematics. Springer: Berlin, 1977.
6. Cullen MJP. Integration of the primitive barotropic equations on a sphere using the finite element method. *Quarterly Journal of the Royal Meteorological Society* 1974; **100**:555–576.
7. Heinze T, Hense A. The shallow water equations on the sphere and their Lagrange–Galerkin-solution. *Meteorology and Atmospheric Physics* 2002; **81**:129–137.
8. Heikes R, Randall DR. Numerical integration of the shallow-water equations on a twisted icosahedral grid. Part I: Basic design and results of tests. *Monthly Weather Review* 1995; **123**:1862–1880.
9. Ringler TD, Randall DA. A potential enstrophy and energy conserving numerical scheme for solution of the shallow-water equations a geodesic grid. *Monthly Weather Review* 2002; **130**:1397–1410.
10. Thuburn J. A PV-based shallow-water model on a hexagonal-icosahedral grid. *Monthly Weather Review* 1997; **125**:2328–2347.
11. Almgren AS, Bell JB, Colella P, Howell L, Welcome ML. A conservative adaptive projection method for the variable density incompressible Navier–Stokes equations. *Journal of Computational Physics* 1998; **142**:1–46.
12. Bonaventura L, Rosatti G. A cascadic conjugate gradient algorithm for mass conservative, semi-implicit discretization of the shallow water equations on locally refined structured grids. *International Journal for Numerical Methods in Fluids* 2002; **40**:217–230.
13. Nicolaides RA. Direct discretization of planar div-curl problems. *SIAM Journal on Numerical Analysis* 1992; **29**:32–56.

14. Quiang D, Gunzburger MD, Lili J. Voronoi-based finite volume methods, optimal Voronoi meshes and PDEs on the sphere. *Computational Methods in Applied Mechanical Engineering* 2003; **192**:3933–3957.
15. Lin SJ, Rood RB. An explicit flux-form semi-Lagrangian shallow water model on the sphere. *Quarterly Journal of the Royal Meteorological Society* 1997; **123**:2477–2498.
16. Williamson DL, Drake JB, Hack JJ, Jakob R, Swarztrauber RN. A standard test set for numerical approximations to the shallow water equations in spherical geometry. *Journal of Computational Physics* 1992; **102**:221–224.
17. Jakob-Chien R, Hack JJ, Williamson DL. Spectral transform solutions to the shallow water test set. *Journal of Computational Physics* 1995; **119**:164–187.

